Materials Science-Poland, Vol. 24, No. 4, 2006

Effect of calcination and structural additives on the EPR spectra of nanocrystalline cobalt oxides

N. GUSKOS[1, 2*], J. TYPEK[2], M. MARYNIAK[2], G. ŻOŁNIERKIEWICZ[2], M. PODSIADŁY[3], W. ARABCZYK[3], Z. LENDZION-BIELUŃ[3], U. NARKIEWICZ[3]

[1]Solid State Physics, Department of Physics, University of Athens, Panepistimiopolis, 157 84 Zografos, Greece

[2]Institute of Physics, Szczecin University of Technology, al. Piastów 17, 70-310 Szczecin, Poland

[3]Institute of Chemical and Environment Engineering, Szczecin University of Technology, Pułaskiego 10, 70-322 Szczecin, Poland

Samples of nanocrystalline Co_3O_4 were prepared at various calcination temperatures and with various amounts of structural additives (CaO and Al_2O_3). The samples were characterized by X-ray diffraction. The average size and size distribution of nanoparticles have been calculated. Electron paramagnetic resonance (EPR) spectra of the samples were recorded at room temperature. The spectra have been attributed to divalent cobalt ions. Samples calcinated at higher temperatures showed an almost symmetrical, intensive EPR line. Temperature of calcination determined the character of the EPR spectra. The intensities of EPR spectra depended on the presence of CaO and Al_2O_3 additives.

Key words: *EPR; cobalt oxide*

1. Introduction

Preparation, characterization and application of some transition metal oxides, such as cobalt oxide, have attracted an increasing interest due to their physical properties as well as rich technological applications. Cobalt oxides, due to their magnetic and catalytic properties, are used in a wide range of applications in various fields of industry, including catalyst, pH sensors, gas sensors and magnetic materials [1–6]. Many methods have been used in recent years to prepare Co_3O_4: sol-gel route [7, 8], reduction-oxidation route [9], cobalt salt decomposition [10–13], chemical vapour deposition [14], electrochemical and sonochemical synthesis [15] and pulsed laser deposition [16]. In particular, methods of obtaining nanocrystaline Co_3O_4 are very important, because the properties of Co_3O_4 are highly sensitive to the particle sizes as well as to

*Corresponding author, e-mail: ngouskos@phys.uoa.gr

the concentrations of defects or other phases. Crystals of the above compound with a normal spinel structure (similar as Fe_3O_4) form two sublattices with different valences of cobalt ions, one with cobalt(II) ions in the ground state $^4A_2$ (high spin, $S = 3/2$) in tetrahedral A sites and the other with cobalt(III) ions in the ground state $^1A_{1g}$ (low spin, non-magnetic, $S = 0$) occupying octahedral local lattice [17, 18]. The high-spin state could be stabilised by cation vacancies in the B sublattice. The concentration of oxygen on the surface of Co_3O_4 could be different from that in the bulk [19, 20]. In transition metal compounds, in particular those containing iron(II) and cobalt(III), spin-state transitions between the low-spin- and the high-spin states occur. Electron paramagnetic resonance (EPR) is one of the most effective methods to study the influence of defects on the physical properties of Co_3O_4 [21, 22]. The conditions of preparation have a strong influence on the transition to disorder and magnetic ordered state [23].

The aim of this report is the EPR study of nanocrystalline Co_3O_4 obtained at various calcination temperatures and with various concentrations of structural additives (CaO and Al_2O_3). The differences in the EPR spectra have been correlated with the presence of additives and calcination temperatures.

2. Experimental

The starting materials were $Co(NO_3)_2 \cdot 6H_2O$, $Ca(NO_3)_2 \cdot 4H_2O$, $Al(NO_3)_3 \cdot 9H_2O$ and 25% solution of NH_4OH. The nitrate salts of cobalt, calcium and aluminium were dissolved in distilled water and NH_4OH was added. Two kinds of cobalt hydroxides were precipitated: one with lower concentrations of promoters (samples P) and other with higher concentration of promoters (samples P′). The precipitated cobalt hydroxides were washed with distilled water and dried at 70 °C to obtain the precursor. The precursor P was calcined at 500 °C for 1 h and at 900 °C for 3 h to prepare Co_3O_4 nanoparticles used to obtain samples P1 and P3, respectively. The precursor P′ was calcined at 900 °C for 3 h and was used to prepare samples P2. Co_3O_4 was characterized by X-ray diffraction (XRD, Philips, X'Pert Pro equipment, $Cu_{K\alpha}$ radiation).

The average crystal size of the nanoparticles was calculated from diffraction peak half-widths using the Scherrer formula. Grain size distribution has been calculated by FW(1/5)/(4/5) method. The concentration of CaO and Al_2O_3 in Co_3O_4 was determined using an inductively coupled plasma-atomic emission spectroscopy (ICP-AES, JY 238 Ultrace equipment from Jobin Yvon). The concentration of structural additives in samples P1 and P3 was the same, while sample P2 contained a greater amount of promoters (Table 1).

The EPR measurements were carried out with a conventional X-band ($\nu = 9.43$ GHz) Bruker E 500 spectrometer with 100 kHz magnetic field modulation. The samples in the form of loose powders, each containing around 30 mg of the substance, were placed into 4 mm diameter quartz tubes.

3. Results and discussion

The concentrations of structural additives (CaO and Al_2O_3) in the samples, as well as mean crystallite sizes determined from the Scherrer formula and from the size distributions (Fig.1), are given in Table 1. As could be expected, the calcination temperature has a crucial influence on the mean crystallite size. Sample P1 calcined at 500 °C consists of crystallites with the mean crystallite size of about 56 nm, while in samples P2 and P3, calcined at 900 °C, the crystallite sizes are twice larger.

Table 1. The concentrations of structural additives and the crystallite diameters (d and D). The parameter σ is the dispersion of crystallite sizes

Sample	Calcination	Promotor concentration		Scherrer analysis	FW(1/5)/(4/5) analysis	
		CaO [wt. %]	Al_2O_3 [wt. %]	d [nm]	D [nm]	σ [nm]
P1	500 °C (1h)	1.2	2.1	56	48	16
P2	900 °C (3 h)	1.7	2.3	>100	–	–
P3	900 °C (3 h)	1.2	2.1	>100	–	–

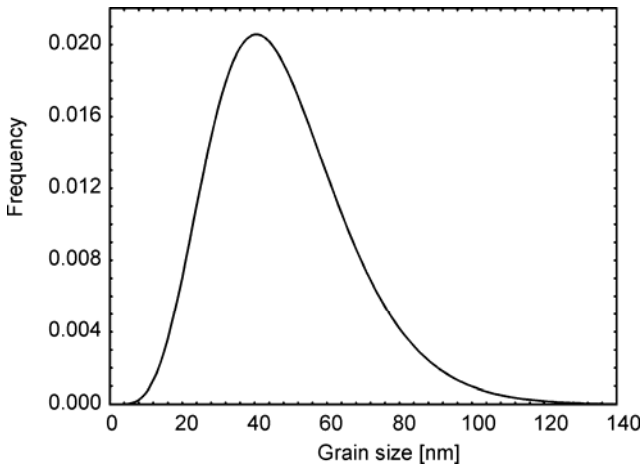

Fig. 1. Grain size distribution of Co_3O_4 (sample P1)

It was also possible to calculate the grain size distribution in sample P1 by the FW(1/5)/(4/5) method. The detailed mathematical procedure is presented elsewhere [24, 25]. The average grain size calculated by this method is 48 nm and is smaller than the value calculated by the Sherrer's method (56 nm). The dispersion of crystallite sizes σ is 19 nm. The grain size distribution is presented in Fig. 1. It could be seen that the majority of the Co_3O_4 crystallites have grain sizes in the range of 15–90 nm. The maximum of the distribution is observed at 40 nm.

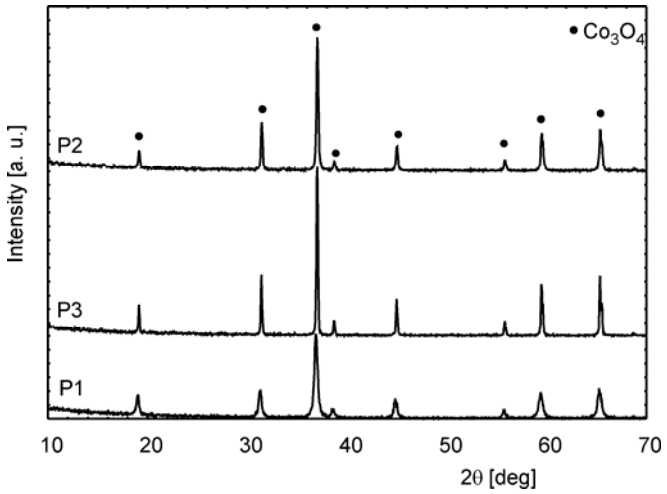

Fig. 2. XRD patterns for the three investigated samples of Co_3O_4 particles

The XRD patterns of Co_3O_4 particles after calcination at various temperatures for the studied samples are shown in Fig. 2. In all the samples the lines from the Co_3O_4 phase dominate the diffraction patterns. Co_3O_4 crystallises in the cubic system, space group $Fd\bar{3}m$, with the lattice parameter a = 8.084 Å.

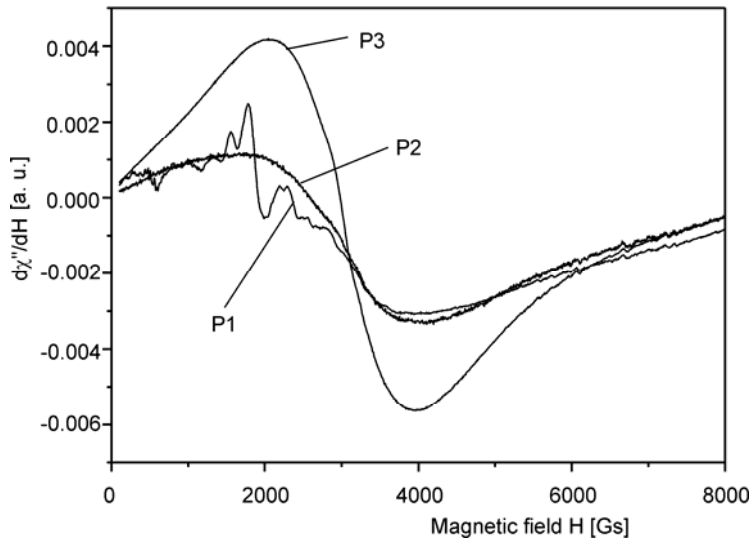

Fig. 3. EPR spectra of the investigated samples at room temperature

Figure 3 presents the EPR spectra of all investigated samples recorded at room temperature. Significant differences in the spectra have been observed between three samples. For the precursor P no EPR signal was recorded while the precursor P′ has shown the EPR spectrum of cobalt(II) ions with a hyperfine structure. The EPR spec-

trum of sample P1 is a superposition of contributions from two paramagnetic centres, one displaying the hyperfine structure and the other producing a very broad line. The amount of structural additives is greater for sample P2 than for sample P3 (Table 1) but the EPR spectrum is more intense for sample P3. An intense, slightly asymmetric line is recorded for both samples P2 and P3 and the resonance line could be fitted by the Lorentzian function including the tail of the resonance absorption at negative fields due to the linearly polarized radio frequency field.

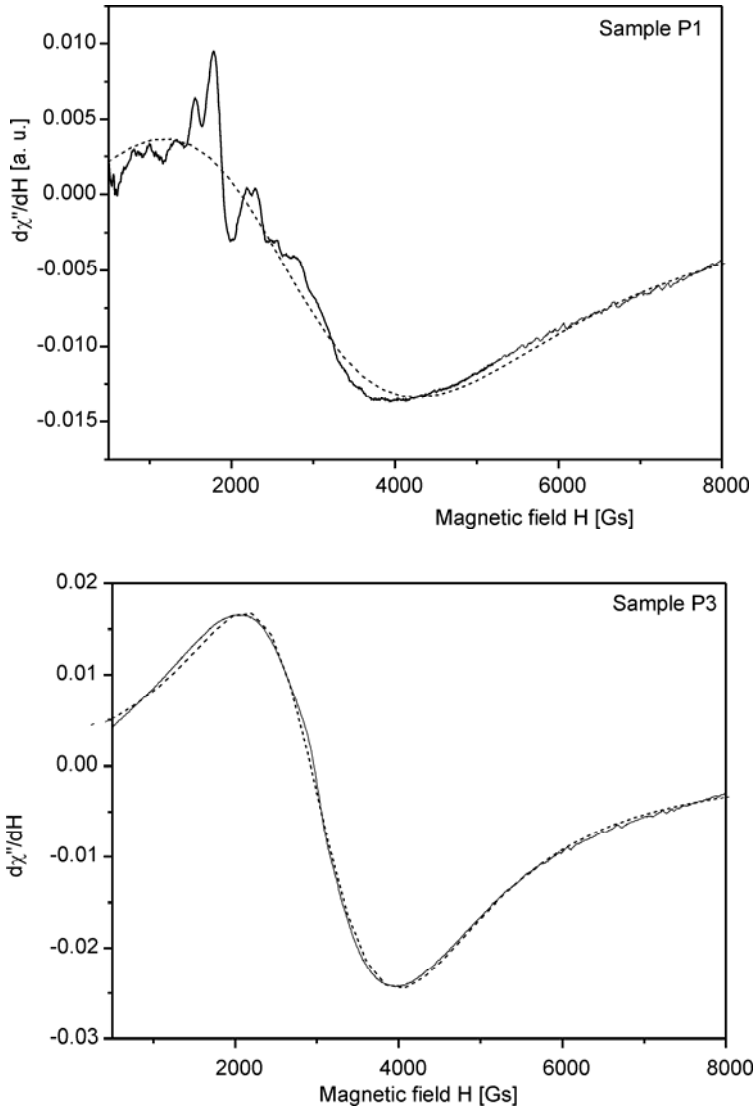

Fig. 4. The fitted (dotted lines) and experimental (solid lines) EPR spectra of sample P1 and sample P3

The results of fitting the EPR spectra of samples P1 and P3 are shown in Fig. 4. In both cases, only the Lorentzian function for the EPR line centred at higher magnetic field has been used. A reasonable fit is obtained for samples P3 and P2 with the resonance line centred at $g = 2.22(1)$ and $g = 2.71(1)$, having the linewidth $\Delta H = 1630(9)$ Gs and $\Delta H = 2070(9)$ Gs, respectively. The EPR line at higher magnetic field for sample P1 is centred at $g = 2.52(1)$ with the linewidth $\Delta H = 1810(10)$ Gs. An additional EPR spectrum with a hyperfine structure appeared in sample P1 at $g_{\text{eff}} = 3.5(1)$.

While cobalt(II) ions at the tetragonal sites in the spinel lattice should produce a single EPR line with the Lorentzian lineshape and with the g-factor of about 2.25 [22], often strongly asymmetric lines with effective g-values $4 > g_{\perp} > 3.5$ and $g_{\parallel} \approx 2$ are observed. The linewidth depends very strongly on the sample thermal preparation processes and increases with decreasing calcination temperature [22]. In this system, the quenching conditions are very important for the very existence of the cobalt(II) EPR signal. A slow cooling of the sample results in the disappearance of the EPR spectrum while doping by other ions could essentially change the intensity of the EPR signal [21].

Low annealing temperature of the sample results in the EPR spectrum that is a superposition of signals from two different paramagnetic centres (sample P1 – Fig. 3) while high annealing temperature of the sample produces the EPR spectrum consisting of one very broad line. In all three cases, the EPR spectra could be regarded as originating from two kinds of paramagnetic entities, suggesting that during the synthesis two kinds of paramagnetic centres were formed. The structural additives could give two different additional phases (Table 1) and they contribute to the EPR spectra of cobalt(II) ions. For low concentration of additives and low annealing temperature (sample P1), the EPR spectrum is composed of two much different paramagnetic centres of cobalt(II) ions (Fig. 4a), while for high annealing temperature mainly one very broad line is observed. At higher concentration of structural additives (sample P3), the EPR spectrum is dominated by a very intense line which probably conceals the other weaker line (Fig. 4b). It could be considered that the EPR linewidth is determined by the cobalt(II) ions spin relaxation time rather than the presence of, e.g., dipolar and isotropic exchange interactions that could produce an exchange narrowed line with the Lorentzian lineshape in the centre of the line [26, 27]. The peak-to-peak width of the resonance line would be approximately given by:

$$\Delta H_{pp} = \frac{2}{\sqrt{3}} \frac{M_2}{H_{ex}} \tag{1}$$

where H_{ex} is the exchange field and M_2 is the second moment of the line, with M_{2d} being the dipole-dipole interaction, M_{2hf} – the hyperfine structure interaction and M_{2f} – the fine structure interaction. These interactions, for a sample in a powder form, could be related by the following formulas:

$$M_{2d} = \frac{3}{4} S(S+1) g^2 \mu_B^2 \sum_j r_{jk}^{-6} \tag{2a}$$

$$M_{2hf} = \frac{1}{3} A_{hf}^2 I(I+1) \tag{2b}$$

$$M_{2f} = \frac{1}{5} \left(4S(S+1) - 3\right) D^2 \tag{2c}$$

The dipole-dipole interactions between magnetic moments of cobalt ions was estimated to have the value of $M_{2d} = 2.6 \times 10^6$ Gs^2 and the hyperfine interaction $M_{2hf} \approx 5.25 \times 10^4$ Gs^2 with $H_{ex} \approx 3 \times 10^5$ Gs [22]. These two interactions (Eqs. (2a) and (2b)) could not explain the observed values of the linewidths in our spectra.

For cobalt(II) ions placed in a near tetrahedral surrounding, the main contribution to the linewidth arises from the splitting of the ground spin quartet due to the deviation of the local crystal fields from the cubic symmetry. Such a deviation should lead to the appearance of term $H_f = D\Sigma_i (S_{iz})^2$ in the spin Hamiltonian and the contribution to the second moment given by Eq. (2c). By the procedure described in Ref. [22], the following values of M_{2f} have been obtained: 4.15×10^8 Gs^2 for sample P3, 5.27×10^8 Gs^2 for sample P2 and 4.61×10^8 Gs^2 for sample P1. The EPR spectrum of tetrahedral cobalt(II) ions in Co_3O_4 is extremely sensitive to the disorder created in the bulk of the crystallites both by the bulk defects and the grain boundary layers, containing the part of the oxygen prevailing in excess of the stoichiometric amount [22]. As is well known, the integrated intensity of the EPR spectrum, proportional to the product of linewidth ΔH and line amplitude I, is directly related to the number of paramagnetic centres. Thus comparison of integrated intensities of the investigated samples could give information on relative influence of the annealing temperature and the structural additives on the amount of paramagnetic centres. The values of the relative ratio of the EPR integrated intensities

$$\frac{(\Delta H_{P3})^2 I_{P3}}{(\Delta H_{P1})^2 I_{P1}} = 1.78 \quad \text{and} \quad \frac{(\Delta H_{P3})^2 I_{P3}}{(\Delta H_{P2})^2 I_{P2}} = 1.24$$

suggest an essential increase of the concentration of cobalt(II) ions in a deformed crystal field in sample P3.

4. Conclusions

The EPR spectra of Co_3O_4 samples strongly depend on the calcination temperature and on the concentration of structural additives. For the precursor P the EPR spectrum of cobalt(II) ions was not observed while for the precursor P′ an intense EPR spec-

trum of cobalt(II) with the hyperfine structure was recorded. An increase of concentration of structural additives (30% increase for CaO and 9% for Al_2O_3) increases the EPR integrated intensity of 1.24 times while higher annealing temperature increase by 1.78 the concentration of paramagnetic cobalt(II) in low symmetry of the crystal field. Two kinds of EPR spectra of cobalt(II) ions were observed: one without a hyperfine structure and the second one with a very broad line for sample P1.

References

[1] JANSSON J., PALMQVIST A.E.C., FRIDELL E., SKOGLUNDH M., OSTERLUND L., THORMAHLEN P., LANGER V., J. Catal., 211 (2002), 387.
[2] QINGWEN L., GUOAN L., YOUQIN S., Anal. Chim. Acta, 409 (2000), 137.
[3] YANG H., HU Y., ZHANG X., QIU G., Mater. Lett., 58 (2004), 387.
[4] HAYASHI E., IWAMATSU E., BISWAS M.E., SANADA Y., AHMED S., HAMID H., YONEDA T., Appl. Catal. A, 179 (1999), 203.
[5] MORALES U., CAMPERO A., SOLORZA-FERIA O., J. New Mat. Electr. Systems, 2 (1999), 89.
[6] MAKHLOUF S.A., J. Magn. Magn. Mater., 246 (2002), 184.
[7] SVEGL F., OREL B., GRABEC-SVEGL I., KAUCIC V., Electrochim. Acta, 45 (2000), 4359.
[8] BARRERA E.C., VIVEROS T.G., MORALES U., Renew. Energy, 9 (1996), 736.
[9] NI Y., GE X., ZHANG Z., LIU H., ZHU Z., YE Q., Mat. Res. Bull., 36 (2001), 2383.
[10] ARDIZZONE S., SPINOLO G., TRASATTI S., Electrochim. Acta, 40 (1995), 2683.
[11] FURLANETTO G., FORMARO L., J. Colloid Interface Sci., 170 (1995), 169.
[12] SATO M., HARA H., KURITANI H., NISHIDE T., Sol. Energy Mater. Sol. Cells, 45 (1997), 43.
[13] VERELST M., ELY T.O., AMIENS C., SNOECK E.,. LECANTE E., MOSSET A., RESPAUD M., BROTO J.M., CHAUDRET B., Chem. Mater., 11 (1999), 2702.
[14] GAUTIER J.L., RIOS E., GRACIA M., MARCO J.F., GANCEDO J.R., Thin Solid Films, 311 (1997), 51.
[15] VIJAYA KUMAR R., DIAMANT Y., GEDANKEN A., Chem. Mater., 12 (2000), 2301.
[16] KOSHIZAKI N., NARAZAKI A., SASAKI T., Scripta Mater., 44 (2001), 1925.
[17] WILL G., MASCIONANI N., PARRISH W., HART M., J. Appl. Cryst., 20 (1987), 394.
[18] SMITH W.L., HOBSON A.D., Acta Cryst. B, 29 (1973), 362.
[19] MARCUS-SAUBAT B., BEAUFILS J.P., BARBAUX Y., J. Chim. Phys., 83 (1986), 317.
[20] BELOVA J.D., ZAV'YALOV S.A., ROGINSKAYA Y.E., Russian J. Phys. Chem., 60 (1986), 140.
[21] STOYANOVA R., ZHECHEVA E., ANGELOV S., Mat. Chem. Phys., 26 (1990), 239.
[22] ANGELOV S., ZHECHEVA E., STOYANOVA R., ATANASOV M., J. Phys. Chem., Solids, 51 (1990), 1157.
[23] BRABERS V.A.M., BROEMME A.D.D, J. Magn. Magn. Mater., 104–107 (1992), 405.
[24] PIELASZEK R., J. Alloys Comp., 382 (2004), 128.
[25] PIELASZEK R., Ph. D. thesis, Faculty of Physics, Warsaw University, 2003.
[26] VAN VLECK J.H., Phys. Rev., 74 (1948), 1168.
[27] ANDERSON P.W., WEISS P.R., Rev. Mod. Phys., 25 (1953), 269.

Received 9 September 2005
Revised 24 November 2005